

OPERATIONAL MAPPING OF THE ENVIRONMENTAL CONDITION OF RIPARIAN ZONES OVER LARGE REGIONS FROM AIRBORNE LIDAR DATA

K. Johansen^{a, b, c}, L. Arroyo^{a, b} and S. Phinn^{a, b}

^a Joint Remote Sensing Research Program - (k.johansen, l.arroyomendez, s.phinn)@uq.edu.au

^b Centre for Remote Sensing and Spatial Information Science, School of Geography, Planning and Environmental Management, University of Queensland, Brisbane, QLD 4072, Australia

^c Centre for Remote Sensing, Dept. of Environment and Resource Management, 80 Meiers Rd, QLD 4068, Australia

KEY WORDS: Riparian Zones, LiDAR, Large Spatial Extents, Riparian Condition, Operational Mapping, Victoria Australia

ABSTRACT:

Riparian zones maintain water quality, support multiple geomorphic processes, contain significant biodiversity and also maintain the aesthetics of the landscape. Australian state and national government agencies responsible for managing riparian zones are planning missions for acquiring remotely sensed data covering the main streams in Victoria, New South Wales, and parts of Queensland and South Australia. The objectives of this paper are to: (1) assess the ability of LiDAR data for mapping the environmental condition of riparian zones; and (2) provide specifications for capturing and analyzing the LiDAR data for riparian zone mapping at large spatial extents (> 1000 km of stream length). LiDAR derived digital elevation models, terrain slope, intensity, fractional cover counts and canopy height models were used for mapping riparian condition indicators using simple algorithms and more complex object-oriented image analysis. The results showed that LiDAR data can be used to accurately map: water bodies (producer's accuracy = 93%); streambed width (Root Mean Square Error (RMSE) = 3.3 m); bank-full width (RMSE = 6.1 m); riparian zone width (RMSE = 7.0 m); width of vegetation (RMSE = 5.6 m); plant projective cover (RMSE = 12%); vegetation height classes (vertical accuracy < 0.20 m); large trees; longitudinal continuity; vegetation overhang; and bank stability ($R^2 = 0.40$). Suitable LiDAR data acquisition specifications are also provided.

1. INTRODUCTION AND OBJECTIVES

Riparian zones along rivers and creeks have long been identified as important elements of the landscape due to the flow of species, energy, and nutrients, and their provision of corridors creating an interface between terrestrial and aquatic ecosystems. Threats to riparian zones are compounded by increased anthropogenic development and disturbances in or adjacent to these environments (Naiman and Decamps, 1997). Conventional field based approaches for assessing the environmental condition of riparian zones are site specific and cannot provide detailed and continuous spatial information for large areas, > 1000 km of streams (Johansen et al., 2007). High spatial resolution image data are required for assessment of riparian zones because of the limited width and the physical form and vegetation structural heterogeneity within riparian zones (Congalton et al., 2002; Johansen et al., 2008). This type of mapping has mostly been applied to riparian study areas of limited spatial extents (< 100 km of stream length) by using high spatial resolution image data. The use of high spatial resolution satellite image data has shown some limitations in deriving riparian condition indicators and do not provide the necessary structural parameters. Light Detection and Ranging (LiDAR) data may be able to provide additional information on riparian condition indicators, but there are currently no examples or set processes for riparian zones (Dowling and Accad, 2003). The objectives of this paper are to: (1) assess the ability of LiDAR data for mapping the environmental condition of riparian zones; and (2) provide specifications for capturing and analyzing the LiDAR data for riparian zone mapping at large spatial extents (> 1000 km of stream length). The specifications of the LiDAR data deemed most suitable for riparian mapping application were also based on results from analysis of LiDAR data of streams and riparian zones in Central Queensland, Australia (Johansen et al., in review).

2. STUDY AREAS AND FIELD DATA

The study area was located along the Werribee and Lerderberg Rivers and Pyrites, Djerriwarrh, and Parwan Creeks in the temperate Werribee Catchment in Victoria, covering approximately 150 km of stream length and associated riparian zones. The Werribee Catchment study area, located 49 km west of Melbourne, included urbanized and cultivated areas along most sections of the streams, but did also comprise a section of state forest in topographically complex terrain (Figure 1).

Field measurements were obtained in the Werribee Catchment from 31 March - 4 April 2008 along transects located perpendicular to the streams of the following parameters: (1) water bodies; (2) streambed, bank-full, riparian zone, and vegetation widths; (3) plant projective cover (PPC); (4) ground cover; (5) vegetation height classes; and (6) bank stability (Johansen et al., 2008). These field parameters were assumed not to have changed significantly between the field and LiDAR data acquisition. Rainfall and stream flow data and riparian field and photo data obtained through the Index of Stream Condition approach (Ladson et al., 1999) from May and June 2004 supported this assumption. For calibration of the LiDAR based object-oriented mapping of streambed, bank-full and riparian zone widths, field data were collected for the bank slope and the elevation difference between the streambed and the external perimeter of the riparian zone. Where possible, existing high spatial resolution optical image data were used to locate in-situ ground control points based on invariant features visible in both the field and image data to complement GPS points to precisely overlay field and image data.

To enable accurate integration of field and LiDAR data, a normalized difference vegetation index (NDVI) produced from a QuickBird multi-spectral image of 2.4 m pixels captured in

June 2006 was geo-referenced to the canopy height model derived from the LiDAR data. Field transect locations were visually located on the QuickBird image by use of GPS and ground control points of features that could be identified both in the field and on the QuickBird image. The location of the field transects were then geometrically adjusted to accurately overlay the QuickBird, and LiDAR data.

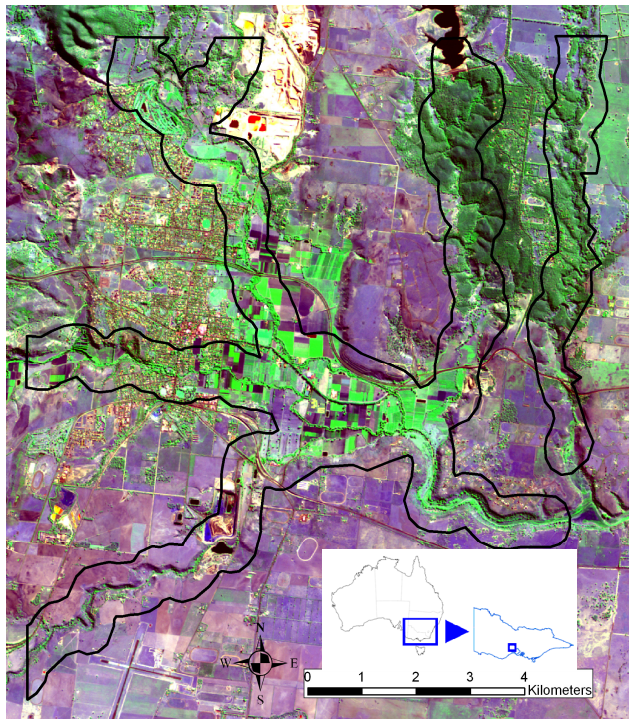


Figure 1. Outline (black line) of study area in Victoria displayed on a SPOT-5 image with a mid infrared, near infrared and red band configuration.

3. METHODS

3.1 LiDAR Data Pre-Processing

Existing LiDAR data captured between 7 and 9 May 2005 were used in this research. The LiDAR data were captured by the Optech ALTM3025 sensor with an average point spacing of 1.6 m (0.625 points per m²) and consisted of two returns, first and last returns, as well as intensity. The LiDAR returns were classified as ground and non-ground by the data provider using proprietary software. The flying height was approximately 1500 m above ground level. The maximum scan angle was set to 40° with a 25% overlap of different flight lines. The estimated vertical and horizontal accuracies were < 0.20 m and < 0.75 m respectively. GPS base stations were used for support to improve the geometric accuracy of the dataset.

3.2 Mapping Riparian Zones from LiDAR Data

Parameters estimated from LiDAR data and used to derive information on riparian condition indicators were: digital elevation model (DEM), terrain slope, variance of terrain slope, fractional cover counts, canopy height model, and intensity (Figure 2). The output pixel size was set to minimize the pixel size and at the same time reduce the number of pixels without data, i.e. pixels without any returns, producing null values. With increased point density, a smaller pixel size could be achieved. The DEM was produced by inverse distance weighted interpolation of returns classified as ground hits. From the DEM, raster surfaces representing terrain slope, rate of change in horizontal and vertical directions from the center pixel of a 3 x 3 moving window, and variance of the terrain slope, within a moving window of 3 x 3 pixels, were calculated. The map of fractional cover counts, defined as one minus the gap fraction probability, was calculated from the proportion of counts of first returns 2 m above ground level to correspond with the field measurements of PPC, which were derived above a 2 m height.

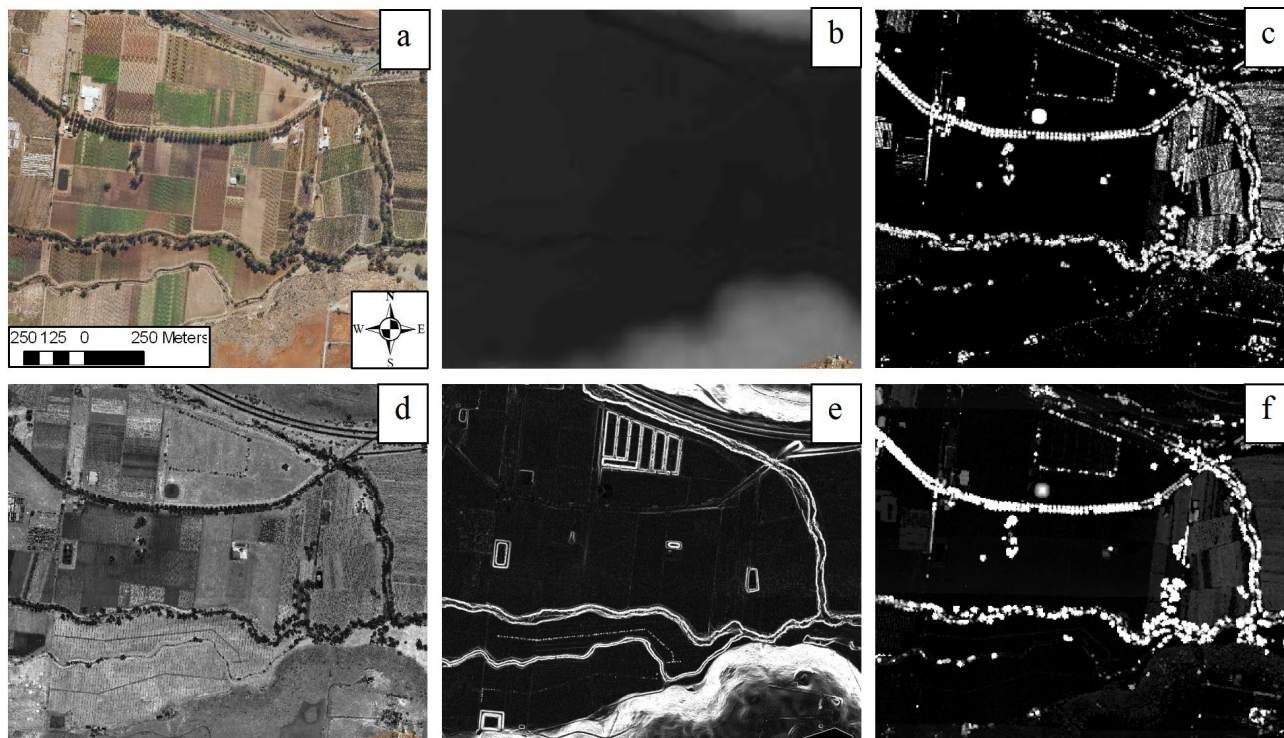


Figure 2: (a) Aerial photograph, and corresponding LiDAR derived raster products, including (b) DEM, (c) fractional cover counts, (d) intensity, (e) terrain slope, and (f) canopy height model. Dark areas = low values and bright areas = high values.

The height of all first returns above the ground was calculated by subtracting the ground elevation from the first return elevation. The maximum height of first returns within each pixel was also calculated. The maximum height of first returns can be considered a representation of the top of the canopy in vegetated areas. The intensity band was produced by inverse distance weighted interpolation.

From the LiDAR raster products riparian condition indicators were either derived directly by using simple algorithms or object-oriented methods. Water bodies, streambed width, bank-full width, riparian zone width, and width of vegetation were mapped using image segmentation and object-oriented image classification in Definiens Developer 7.

Water bodies were mapped from the LiDAR data using the intensity, DEM, PPC, and terrain slope bands. A local extrema algorithm was first used to find minimum values from the DEM within a searching range of 15 pixels throughout the LiDAR data extent. Only extreme minimum DEM values with an intensity value < 50 , a PPC value of 0, and a terrain slope $< 2.5\%$ were considered. This result was then used to grow water bodies as long as the neighbouring objects had intensity mean values of less than 100 and a terrain slope $< 2.5\%$ (Figure 3).

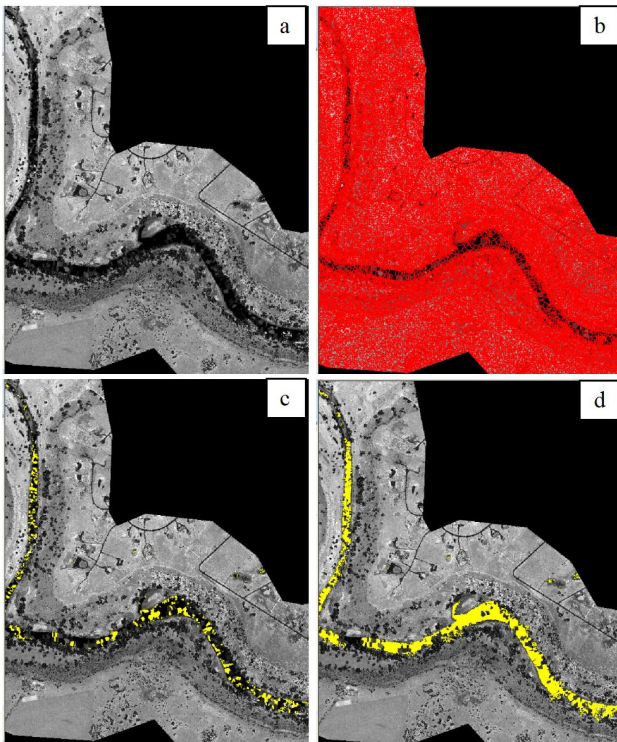


Figure 3. The (a) LiDAR intensity band, (b) the segmentation result, (c) the identification of water bodies (yellow objects), and (d) and region growing mapping result.

The streambed, defined as the area between the toes of the banks, was mapped from the DEM, terrain slope, and the variance of terrain slope using object-oriented image analysis. The multiresolution segmentation process in Definiens Developer 7 was based on the DEM and variance of terrain slope, which produced objects lining up with the gradient of the terrain and producing separate objects for the streambed, stream bank and surrounding areas because of elevation differences. The object-oriented classification of streambeds from the LiDAR data first identified the stream banks based on their steep slopes. Objects of low-lying areas based on the DEM

located in between steep slopes and with borders to other objects with higher elevation were mapped as streambed.

To map bank-full width, defined as the area between the top of the lowest bank on each side of the stream, the streambed map was expanded using a region growing algorithm to grow the streambed extent up to an elevation of 2 m above the current streambed, but limited to a distance from the original streambed of 10 m based on field observations. This expanded the original streambed to include areas belonging to the bank-full width. The next step assumed that the streambed had now been expanded to include at least a small part of the lower stream bank. To reach the top of the lowest bank, the expanded streambed extent was grown further as long as the bank slope was larger than 7%, but bounded by an elevation height of 4 m above the streambed to set an upper threshold above the streambed. This threshold was necessary as some of the riparian areas were surrounded by steep terrain with terrain slopes $> 7\%$.

For mapping the extent of riparian zones, the following input bands were used for the object-oriented image analysis: PPC, canopy height model, terrain slope, DEM, and the streambed classification. The classification of the streambed was used to identify the streamside perimeter of the riparian zone. The classification of the riparian zone was then based on the distance from the streambed, the slope of the stream banks, the PPC, and the height of trees, as an abrupt change in vegetation height, density and bank slope generally occur along the external perimeter of riparian zones (Land and Water Australia, 2002). Unclassified objects within the riparian zone, i.e. riparian canopy gaps, enclosed by objects classified as streambed and riparian zones were also classified as part of the riparian zone. The merged riparian zone polygons were then re-segmented into small objects, and areas, classified as riparian vegetation, with an absolute elevation difference > 5 m in relation to the streambed objects, were omitted, as field data indicated that the top of banks was less than 5 m above the streambed. To map width of vegetation, defined as the perpendicular distance from the streambed to a non-riparian zone or non-woody vegetation pixel, the riparian zone width was merged with adjacent woody vegetation with PPC $> 20\%$.

PPC was estimated from the LiDAR based fractional cover counts. Using the same procedures as Armston et al. (in press), fractional cover counts above a height of 2 m were converted to PPC using a power function. For mapping longitudinal continuity, canopy gaps were defined as an area with less than 20% PPC and a size of $> 10 \times 10$ m. The mapping of vegetation height classes was done in one step by dividing individual pixels into height categories based on the canopy height model. To avoid erroneously including agricultural fields and buildings, height categories were only obtained from those areas classified as riparian zones. Similarly, the area covered by large trees within the riparian zone were mapped as the area of tree crowns or parts of tree crowns above a height of 18 m. Vegetation overhang was mapped using the LiDAR derived streambed map and the pixel based PPC map as input bands. For areas to be classified as vegetation overhang, a minimum of 20% PPC was set as a threshold within areas classified as streambed.

Bank stability was mapped from multiple regression analysis based on the relationship between field assessed bank stability and LiDAR derived PPC and terrain slope. PPC was used as tree roots from woody vegetation stabilize banks. Hence, the more PPC, the more stable banks can be expected. Steep bank terrain slopes may indicate potential for erosion and slumping

and hence relate to bank stability levels (Land and Water Australia, 2002).

3.3 Accuracy Assessment

The mapping accuracies of the riparian condition indicator maps were assessed using the field data. For the maps consisting of continuous data values (e.g. PPC), R^2 values and Root Mean Square Error (RMSE) were calculated. For the thematic map of water, producer's accuracy was calculated using an existing QuickBird image from June 2006. High rainfall rates in February 2005 within the study area were followed by lower than average rainfall till June 2006. As the in-stream water levels were assumed to be lower and cover smaller areas in June 2006 (QuickBird capture) than May 2005 (LiDAR capture), only the probability of reference data points from the QuickBird image being classified correctly in the LiDAR derived map of water bodies was calculated.

3.4 LiDAR Data Specifications

The specifications of the LiDAR data deemed most suitable for riparian mapping applications were based on the riparian condition indicator mapping results from this work as well as research conducted along streams and riparian zones in Central Queensland, Australia (Johansen et al., in review). Specifications were also based on other studies for mapping woody vegetation from LiDAR data (e.g. Armston et al, in press; Goodwin et al., 2006).

4. RESULTS AND DISCUSSION

4.1 LiDAR Derived Riparian Condition Indicator Mapping

The results showed that the use of LiDAR data enabled mapping of a number of the riparian condition indicators with high mapping accuracies and levels of detail. In addition to the LiDAR raster products (DEM, terrain slope, fractional cover counts, canopy height model, and intensity), the following riparian condition indicators were mapped automatically: water bodies; streambed width; bank-full width; riparian zone width; width of vegetation; PPC; longitudinal continuity; vegetation height classes; large trees; vegetation overhang; and bank stability (Figures 3 and 4). Mapping accuracies of the LiDAR based riparian condition indicator maps were derived from field data for the Victoria study sites. Vegetation height classes and location of large trees were not validated because of the high vertical accuracy of the point clouds (< 0.20 m). The producer's accuracy of water bodies assessed against a QuickBird image from June 2006 was 93% (n = 102). Field measurements of streambed (RMSE = 3.3 m, n = 17), bank-full (RMSE = 6.1 m, n = 17) and riparian zone widths (RMSE = 7.0 m, n = 17) were compared directly with the corresponding locations within the maps. PPC was validated against an independent field dataset and had a RMSE of 12% PPC (n = 110). The mapping accuracies of vegetation overhang and longitudinal continuity were derivatives of the streambed and PPC maps. Compared against field data, LiDAR derived bank stability based on the terrain slope and PPC maps was mapped with an $R^2 = 0.40$ using multiple regression analysis.

Several of the indicators of riparian zone condition (PPC; vegetation height classes; large trees; vegetation overhang; and bank stability) could be mapped from traditional per-pixel analysis through use of algorithms developed between field data and the LiDAR derived raster products. Object-oriented image analysis assisted in automatically mapping water bodies,

streambed width, bank-full width, riparian zone width, width of vegetation, and longitudinal continuity to enable development of rule sets taking into account context relationships. The initial mapping of the streambed was required to accurately map bank-full and riparian zone widths as the distance to and location and elevation of the streambed provided useful context information. The initial classification of those land-cover classes easiest to map facilitates mapping of other more complex indicators of riparian zone condition. Field data can also contribute to the training stages of object-oriented image classification.

The use of LiDAR data allow some measurements to be obtained with the same or even higher accuracies than from field surveying (e.g. projective foliage cover and canopy height (Armston et al., 2004)). Field data for calibrating and validating the LiDAR derived maps should cover the full variability of the riparian condition indicators to improve results. For example, for mapping bank stability, it is important that all levels of bank stability are assessed in the field under as many different conditions as possible (e.g. urban, undisturbed, bedrock, alluvial soil, and agricultural conditions for streams with and without in-stream water). Field measurements of streambed, bank-full and riparian zone widths, PPC and bank stability were required for calibration and validation of LiDAR derived maps. For riparian condition indicators showing a large level of spatial heterogeneity, such as PPC and bank stability, differential GPS positioning is essential to ensure precise integration of field and LiDAR data. Coincident airborne image data would be very suitable for calibration and validation of LiDAR based water body classification.

4.2 Specifications for LiDAR Data Acquisition and Analysis

LiDAR sensors designed for corridor mapping, such as the Toposys Harrier 56/G3 Riegl LMS-Q560, were considered most appropriate for cost-effectively and consistently mapping riparian condition indicators for areas > 1000 km of stream length. These systems also enable capture of coincident very high spatial resolution image data on an opportunistic basis when weather conditions permits optical data capture. A low-cost coincident optical image dataset would be appropriate for calibration and validation of LiDAR derived riparian condition indicator maps. The LiDAR data were found very suitable for acquisition and analysis because of consistent scan angles, ability to capture data in cloudy conditions, and capacity for mapping automation. LiDAR specifications deemed most suitable for riparian mapping applications based on the experiences gained for the study sites in Victoria, a study site in Central Queensland and the literature (Goodwin et al., 2006; Armston et al., in press) are presented in Table 1.

Table 1. Some suggested LiDAR data acquisition specifications for riparian mapping applications.

Parameters	Value
Scan angle	≤ 15 degrees
Maximum scan angle	30 degrees
LiDAR overlap between runs	30%
Point spacing	0.50 m along/across track
Point density	> 4 points/m
Spot footprint	≤ 0.30 m
Sensor settings to be reported	Maximum scan angle; pulse rate; scan frequency; X, Y, and Z uncertainty
Format	Las 1.2 to store geo-referenced information without any approximations
Return intensity	Radiometrically calibrated
Point cloud classification	Into ground and non-ground

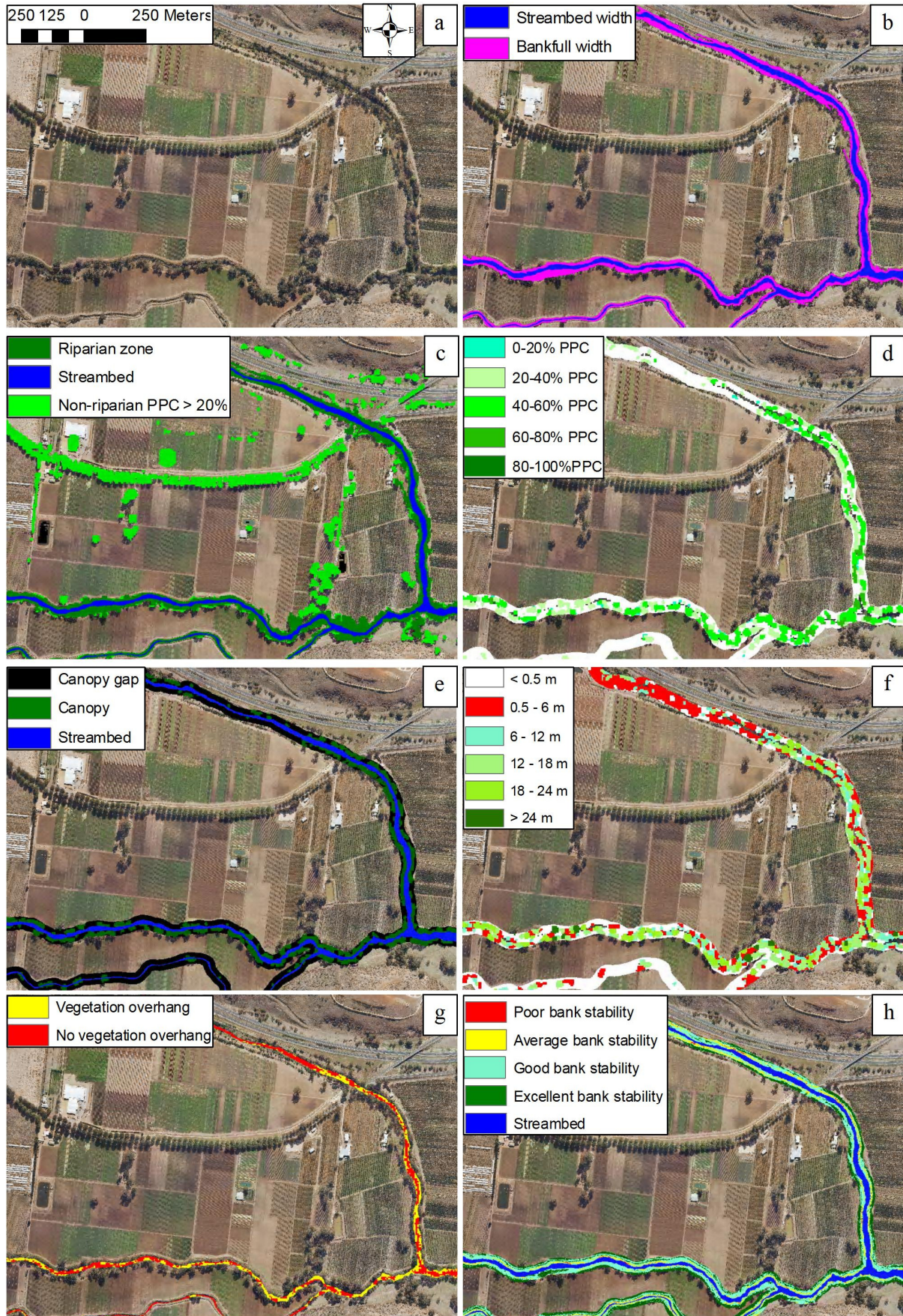


Figure 4. (a) Aerial photograph and associated LiDAR derived maps of (b) streambed and bank-full widths, (c) riparian zone and vegetation widths, (d) PPC, (e) longitudinal continuity, (f) vegetation height classes, (g) vegetation overhang, and (h) bank stability.

As the intrinsic attributes of riparian features being mapped will vary depending on location and the feature being assessed, the extrinsic specifications of the LiDAR data acquisition will need to suit a wide range of requirements. The canopy gap size distribution affects the dynamic range of cover estimates as the LiDAR beam is “blind” to gaps smaller than its cross-sectional area. Previous work over a range of vegetation types has indicated that an average point spacing of < 1 m and a maximum beam cross-sectional diameter < 30 cm will provide good mapping precision up to approximately 70% foliage cover (Armston et al., in press). The scan angle should be minimized (at least < 15°) to limit the effects of leaf angle distribution and ground slope on spatial variation in cover profile estimates in order to avoid more advanced modeling (Goodwin et al., 2006). To obtain information on riparian forest structure at a spatial scale suitable for streams with narrow riparian zones (< 20 m wide), the point density should be at least 4 points / m² (> 0.5 m point spacing). With a set laser beam divergence at 0.5 mrad, a flying height of ≤ 600 m is required to achieve a footprint size of ≤ 30 cm diameter. It is recommended that an area of at least 100 m beyond the external perimeter of the riparian zone on each side of the stream is covered. A total swath width of 500 m would be sufficient for the majority of streams and associated riparian zones in Victoria. To achieve a swath width of 500 m with a scan angle < 15° and a footprint size ≤ 30 cm diameter, two parallel strips with 30% overlap will need to be flown. Pulse Repetition Frequency (PRF) and platform speed are to be determined to optimize point density, the altitude of the platform, the maximum scan angle, and the beam divergence, which, in combination with altitude, dictates the ground footprint size (Goodwin et al., 2006). If possible, the altitude and PRF should be kept consistent to avoid attenuation of the beam with distance and to keep the amplitude and width of the emitted pulse constant. Metadata are required to provide detailed and complete documentation of the acquisition as well as independent accuracy assessment using field data obtained at the time of LiDAR data acquisition. It is also important that specific processing documentation is developed to the extent, where the processing routines can be precisely repeated. This is important for successful future monitoring of streams and riparian zones.

5. CONCLUSIONS AND FUTURE WORK

Our findings show that LiDAR data can be used to accurately map a number of riparian condition indicators over large spatial extents: water bodies; streambed width; bank-full width; riparian zone width; width of vegetation; PPC; longitudinal continuity; vegetation height classes; large trees; vegetation overhang; and bank stability. With suitable acquisition specifications, LiDAR data were found highly suitable for acquisition and mapping of riparian zones for large regions because of consistent scan angles, ability to capture data over shorter time frames, and capacity for mapping automation. Future work will focus on LiDAR mapping applications at the state level in Australia for > 100,000 km of stream length.

REFERENCES

Armston, J.D., Danaher, T.J., and Collett, L.J. (2004). A regression approach to mapping woody foliage projective cover in Queensland with Landsat data. In: *Proceedings of the 12th Australasian Remote Sensing and Photogrammetry Conference*, October 2004, Fremantle, Australia.

Armston, J., Denham, R., Danaher, T., Scarth, P., and Moffiet, T., in press. Prediction and validation of foliage projective cover from Landsat-5 TM and Landsat-7 ETM+ imagery for Queensland, Australia. *Journal of Applied Remote Sensing*.

Congalton, R.G., Birch, K., Jones, R., and Schriever, J., 2002. Evaluating remotely sensed techniques for mapping riparian vegetation. *Computers and Electronics in Agriculture*, 37, pp. 113-126.

Dowling, R., and Accad, A., 2003. Vegetation classification of the riparian zone along the Brisbane River, Queensland, Australia, using light detection and ranging (lidar) data and forward looking digital video. *Canadian Journal of Remote Sensing*, 29(5), pp. 556-563.

Goodwin, N.R., Coops, N.C., and Culvenor, D.S., 2006. Assessment of forest structure with airborne LiDAR and the effects of platform altitude. *Remote Sensing of Environment*, 103(2), pp. 140-152.

Johansen, K., Dixon, I., Douglas, M., Phinn, S., and Lowry, J., 2007. Comparison of image and rapid field assessments of riparian zone condition in Australian tropical savannas. *Forest Ecology and Management*, 240, pp. 42-60.

Johansen, K., Phinn, S., Lowry, J., and Douglas, M., 2008. Quantifying indicators of riparian condition in Australian tropical savannas: integrating high spatial resolution imagery and field survey data. *International Journal of Remote Sensing*, 29(3), pp. 7003-7028.

Johansen, K., Arroyo, L.A., Armston, J., Phinn, S., and Witte, C., in review. Mapping riparian condition indicators in a sub-tropical savanna environment from discrete return LiDAR data using object-based image analysis. *International Journal of GIS*.

Ladson, A.R., White, L.J., Doolan, J.A., Finlayson, B.L., Hart, B.T., Lake, P.S., and Tilleard, J.W., 1999. Development and testing of an index of stream condition for waterway management in Australia. *Freshwater Biology*, 41, pp. 453-468.

Land and Water Australia (2002). *River landscapes; fact sheet*. Land and Water Australia, Canberra, Australia.

Naiman, R.J., Decamps, H., 1997. The ecology of interfaces: riparian zones. *Annual Review of Ecology and Systematics*, 28, pp. 621-658.

ACKNOWLEDGEMENTS

Eric Ashcroft, Michael Hewson and Santosh Bhandari from the Centre for Remote Sensing and Spatial Information Science at University of Queensland, Australia, and Andrew Clark, John Armston, Peter Scarth, Christian Witte, Robert Denham, and Sam Gillingham from the Remote Sensing Centre at QLD Department of Environment and Resource Management, Australia and Paul Wilson, Sam Marwood and John White from the Department of Sustainability and Environment, Victoria provided significant help with fieldwork and image processing. L.A. Arroyo is funded by the Fundacion Alonso Martin Escudero (Spain). K. Johansen is supported by an Australian Research Council Linkage Grant to K. Mengersen, S. Phinn, and C. Witte.